Pulse field magnetisation of bulk high temperature superconductors (GdBCO) with a variety of sample and split coil geometries

MPhys Project: CMP06, CN: 834075, word count: 6380, Supervisor: Prof. Harry Jones

Abstract

Work in the area of flux trapping in bulk high temperature superconductors has shown that the effectiveness of the magnetisation depends on the geometry of the sample – magnetising coil system. Three samples of bulk superconducting GdBCO (two sharing the same diameter and two sharing the same thickness) were magnetised at 77K using the pulse field magnetisation (PFM) technique with multiple pulse runs. A study was carried out to find the effect of changing the relative diameter of the sample and split coil on the efficiency of the magnetisation, for this four split coils of different diameter were constructed. The results show flux trapping is highly dependent on the sample used and field applied but there is little evidence to suggest a dependence on the coil used.

1 Introduction

Trapping flux in melt-processed high temperature superconductor (HTSC) bulks leading to quasi permanent magnets is of interest as they are capable of yielding higher magnetic energy densities [1] than that of conventional permanent magnets. This higher magnetic energy density has many possible applications where a high field permanent magnet is required, for example high powered motors [2, 3], generators for use in wind turbines [4], low friction bearings for fly wheels [5, 6, 7] and applications in NMR systems [8]. The aim of this study is to investigate the parameters of coils and samples that affect the efficiency of magnetisation in a sample, in particular the effect of changing the relative diameters of coil and sample is examined. I will now give a brief history of superconductivity and an account of the phenomenon of flux trapping in superconductors.

1.1 The discovery of superconductivity

Superconductors were first discovered in 1911 by H. Kammerling Onnes [9] when he observed that below a certain critical temperature (4K) mercury's resistivity dropped to exactly zero. As time moved on more materials were found that exhibited this property and in 1986 Bednorz and Muller discovered that $La_{2-x}Ba_xCuO_4$ became superconducting at a much higher critical temperature of 38K [10]. Soon after it was found that a similar compound $YBa_2Cu_3O_7$'s critical temperature was as high as 92K [11]. This study will examine derivatives of these ceramic high temperature superconductors.

1.2 Definition of superconductivity and the Meissner-Ochsenfeld effect

Although a key characteristic of a superconductor is that its resistivity is exactly zero, this is not taken to be the true definition of a superconductor. It was found that a superconductor expels a weak external magnetic field [12], that is if you apply a weak magnetic field to a superconducting material you will find that no field enters. This is called the Meissner-Ochsenfeld effect, it is a separate physical phenomena from zero resistivity and is now taken to be the defining property of a superconductor.

For a superconductor to preserve $\mathbf{B} = 0$ within its boundaries even if there is a small external field present it must have screening currents flowing around the outside of the sample [13, p54], these will produce a magnetic field equal and opposite to the field applied, and will cancel leaving zero field in the superconductor. The screening currents $\mathbf{j}_{screening}$ produce a magnetisation $\mathbf{M} = \nabla \times \mathbf{j}_{screening}$ per unit volume in the sample and with $\mathbf{H}$ defined as the magnetic field due to the external currents only $\mathbf{H} = \nabla \times \mathbf{j}_{external}$. We find that the relation $\mathbf{B} = \mu_0(\mathbf{M} + \mathbf{H})$, and $\mathbf{B} = 0$ imply $\mathbf{M} = -\mathbf{H}$. This is the definition of perfect diamagnetism.

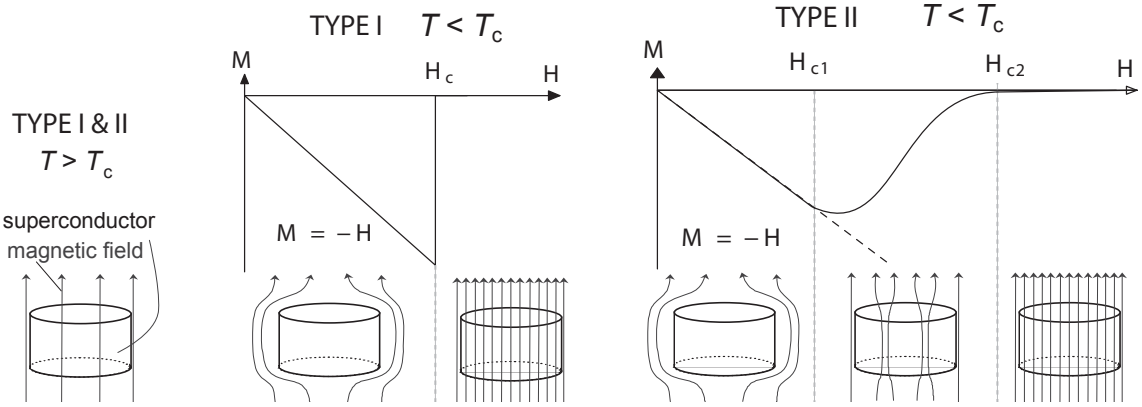

Figure 1 – Superconductors in a external magnetic field. Magnetisation curves of type I & II superconductors showing region between H_{c1} and H_{c2} in which flux can enter a Type II superconductor. Images adapted from James F. Annet and G. Krabbes [13, p57][14, p4].

1.3 Type I and type II superconductors

There are two types of superconductors, named Type I and Type II, they differ from one another in their response to an increasing external magnetic field, seen in figure 1. In the case of a Type I superconductor, the B field will stay at zero inside for small external magnetic fields (due to the Meissner-Ochsenfeld effect, with $\mathbf{M} = -\mathbf{H}$). Then at a certain critical magnetic field H_c the superconductive state will be destroyed and the material will return to its normal (non-superconducting) state $\mathbf{M} = 0$. For a Type II superconductor [14, p1] there are 2 critical fields, below the 1^{st} critical field H_{c1}, $\mathbf{B} = 0$ inside the superconductor with $\mathbf{M} = -\mathbf{H}$ but then at H_{c1} magnetic flux does begin to penetrate the superconductor ($\mathbf{B} \neq 0$) and $\mathbf{M} > -\mathbf{H}$. As the magnetic field applied increases $\mathbf{M}$ approaches zero until the applied field reaches the 2nd critical level H_{c2} at which point $\mathbf{M} = 0$ and the the material stops superconducting.

1.4 Vortices, flux pinning and flux creep

In the phase between H_{c1} and H_{c2} flux can enter the superconductor. Abrikosov gave a physical explanation of this [15] showing that circulating super currents are set up around normal (non superconducting) cores in the material. It is in each of these normal regions of the material that a quantum of magnetic flux can enter [14, p3] with the circulating current shielding the rest of the superconductor from these flux lines. The number of these lines that are parallel to the applied magnetic field increase with field until H_{c2} where the material becomes normal. The magnetisation is reversible (flux can't be trapped) in defect free type II superconductors due to the motion of the normal regions under the Lorentz forces present. In type II superconductors with defects, normal regions can minimize their energy by forming near impurities in the material. They are then 'pinned' to these sites, which limits the motion due to the Lorentz forces. In this case the magnetisation is no longer reversible, allowing flux to be trapped in the superconductor. Thermally activated flux creep can occur dissipating this trapped flux, see [14, p11] for details.

There are several methods for magnetising a sample, the pulse field magnetisation (PFM) technique will be used in this study where magnetising coils are pulsed with a high current for a short length of time generating large fields using small coils. PFM has several advantages over static field methods [16]; it is inexpensive, uses simple cryogenics and is relatively compact, which allows for magnetisation of a sample to be carried out after it has been mounted into a desired piece of machinery [17].

In [18], simulations were carried out on the effective magnetisation of samples of different radii, these simulations suggest that the magnetisation process is most effective when the outer radius of the coils lie between 100% and 50% of the sample radius. Investigations of the effect of changing relative radii of the sample and coil were carried out to ascertain if this conclusion is apparent in this study. For this four split (vortex type) coils of different outer diameter will be constructed and used to magnetise three samples of cylindrical GdBCO bulk material.

This report is structured as follows. In section 2 I will outline the design considerations for the coils, their construction and the experimental set up. In section 3 I will detail the properties of the coils produced and go on to discusses the flux trapping capabilities of the coil-sample combinations and in section 4 I will conclude and suggest further work that could be carried out in this area.

2 Method

To be able to compare the effects of changing the radius of the cylindrical sample and coil on the efficiency of flux trapped during a pulse requires coils of different outer radii to be produced. There are many properties of the pulses that need to be taken into consideration, rise time of pulse, dB/dt during rise, duration of pulse and maximum magnetic field produced. These properties depend on the characteristics of both the capacitor bank used to supply the current and of the coils themselves. I will now look at these in detail, in particular on the constraints that are placed on the design of the coils.

2.1 Capacitor bank

The capacitor bank (see figure 2) used to supply the current pulse is made of three capacitors with a total capacitance C of 204mF with the system limited to a voltage of 63V. These capacitors are charged to various voltages V_{cap} using a high voltage power supply (not shown in fig 2). The capacitors are discharged through the split coil by closing the thyristor switch, which supplies the thyristor with a current trigger allowing it to conduct. The thyristor will continue to conduct until the voltage is reversed, protecting the capacitor bank. When the peak current is reached the current flows mostly through the crowbar resistor $R_{crowbar}$ and not through the capacitors.

Current through the coil will be calculated using Ohm's law by measuring the voltage across the shunt resistor (0.01Ω) which is in series with the coil.

When the dump switch is closed the capacitors will discharge into the dump resistors R_{dump} allowing for the dumping of unwanted charge on the capacitor.

When the capacitors are discharging the circuit is modeled as a series RLC circuit, the standard derivation of which can be found in [19] or [20, p191]. The key results are that the current through the coil is given by

$$I(t) = \frac{V_{cap}}{L\omega} \exp(-\alpha t) sin(\omega t) \tag{1}$$

where

$$\alpha = \frac{R_{coil} + R_{shunt}}{2L} \quad \text{and} \quad \omega = \omega_0 \sqrt{1 - \frac{\alpha^2}{\omega_0^2}}$$

with $\omega_0 = 1/\sqrt{LC}$ (the angular frequency of a LC circuit). L is the inductance of the split coil pair and $R's$ refer to the various resistances in the circuit see figure 2. The behavior of the current can be in any one of three regimes dependent on the value of the unitless constant $\gamma = \alpha^2/\omega_0^2$. When $\gamma < 1$ the system is said to be under damped , $\gamma = 1$ the system is critically damped an $\gamma > 1$ the system is said to be over damped.

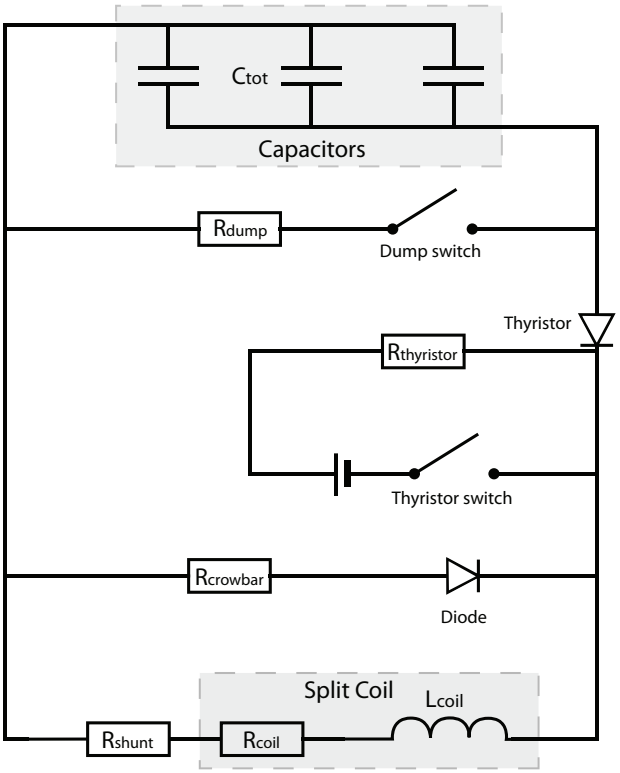

Figure 2 – Circuit diagram of capacitor bank and split coil system.

The rise time of the circuit is the time taken to reach the peak I which is given by

$$t_{rise} = \frac{1}{\omega} arctan(\frac{\omega}{\alpha}) \tag{2}$$

[20, p192] and the peak current is given by $I(t = t_{rise})$:

$$I_{max} = \frac{V_{cap}}{L\omega} \exp(-\alpha t_{rise}) sin(\omega t_{rise}) \tag{3}$$

The discharge of the coil through the crowbar can be approximately modeled as an LR circuit. The current as a function of time is given by a decaying exponential

$$I(t) = I_{max} \exp\left[-\frac{R_{Coil} + R_{Crowbar}}{L} t\right] \tag{4}$$

These are the equations governing the current in the circuit.

2.2 Magnet Design

A split coil (two identical coaxial multi-layered solenoids with a gap between them, see figure 4 and cross section in figure 5) will be used so that comparisons can be made to Xu's [18] work. A split coil arrangement is of interest to those working in flux trapping in HTSC as it has some practical advantages over a simple multi-layered solenoid. Cooling the sample is more efficient [18] which is important as temperature change during the flux trapping process causes thermally activated flux creep. In a simple solenoid it is usual to insert the sample into the bore of the magnet, which requires the bore diameter to be larger than that of the sample diameter, this limits the achievable field and is not a concern in a split coil arrangement. Also there is a very different mechanism of flux penetration between these two types of coil as studied in [21], this is due to the flux entering from the top and bottom surfaces in the split coil case rather than from the periphery in the solenoid case [22]. It has been shown that by using a split coil arrangement the total trapped flux has been made to increase by 30% [23] compared to PFM using conventional solenoids. The split coil will comprise of two identical solenoids as simulations in [18] suggest this is the optimum arrangement for efficient flux trapping.

To carry out a study on how the trapped flux varies with the ratio of coil diameter to sample diameter, magnets of different outer diameters needed to be produced. It was important to fix some of the properties between the coils so comparisons between the different geometries could be made independently of other possible factors. A simulation using split coils has shown that rise time has little effect on the flux trapping capabilities [24] but there have been studies that show the rise time of a pulse has a large effect on the trapped flux [25] and that it is just the rise time, and not the entire pulse length that is important. In this experiment it was decided to keep the rise times constant between the coils, so that if rise times do effect the trapping this wouldn't be a factor when comparing data from different coils. These coils will then produce a range of different maximum magnetic fields, so to be able to compare results from different coils I plan, if possible, to examine the fraction of trapped to applied field for different runs and also runs that apply approximately the same magnetic field.

The quantity dB/dt during the rise of a pulse may also be important, if rise times are matched and coils apply the same magnetic field B_{max}, B_{max}/t_{rise} will also be the matched.

	Samp1	Samp2	Samp3
Diameter /mm	20.7	26.2	26.4
Thickness /mm	9.77	9.95	13.56
Coil A	0.57	0.45	0.45
Coil B	0.94	0.74	0.74
Coil C	1.28	1.01	1.00
Coil D	1.81	1.43	1.42

Table 1 – Cylindrical GdBCO sample diameters and thicknesses. Ratios of outer coil diameters to sample diameters range from 0.45 - 1.81

Matching the rise times of the full LCR expression (equation 2) and keeping other properties like resistance, max current produced and magnetic field applied by the coil is a difficult optimisation problem. It was decided, due to time constraints, to match the rise time by matching the inductance of the coils and then match the resistances by adding resistors in series with the coils. Performing experiments on both the coils with and without resistors will give us a wealth of data to analyse the effects of other properties of the coils.

The inductance of a split coil pair was set to 600μH giving, in the case of negligible resistances, a rise time of of 8.7ms. In the design of these coils the mutual inductance between the two coils was ignored as this effect contributes <1% [20].

We were interested in having the bore size as small as possible, thus maximizing the field produced but a compromise had to be reached as there were practical limitations in winding the coils. First for larger diameter wire it becomes increasingly difficult to wind around a small diameter bore, and second, the former itself has to be able to withstand an appreciable force whilst winding. After some winding tests it was decided that a 4mm bore diameter was the minimum we could safely use.

We required a large spread in the outer diameters of coils relative to the diameter of the samples used. Xu's paper [18] suggests that the outer diameter of the coil should lie between 50% - 100% the diameter of the sample. In this study we would like to look at a range larger than this to see if there is an appreciable drop off in efficiency above or below the optimal region stated. We choose a range about 40% - 180% and decided on outer diameters for the coils which would cover this range (see table 1 & 2).

We used a program that uses an adaption of Wheeler's approximation for a multilayer air core inductor [26]

$$L = \frac{31.6N^2a^2}{6a + 9l + 10c} \tag{5}$$

	Coil A	Coil B	Coil C	Coil D	Departures
inner diameter /mm	4	4	4	4	~ 8%
outer diameter /mm	12.14	20.28	26.8	37.53	2%
length /mm	75	11.2	14	34	$+2w_d$, 2%
number of turns	663	198	176	196	±16 turns
w_d wire diameter /mm	0.68	0.68	0.95	1.68	
inductance per coil / μH	300	300	300	300	35%

Table 2 – Design parameters of single coils. Last column gives rough indication of maximum departures from design in the final coils.

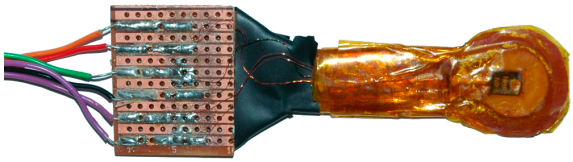

Figure 3 – Hall Probe mount with pickup coil

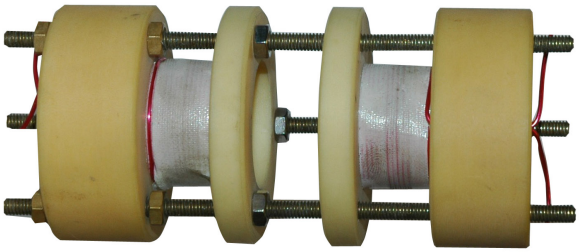

Figure 4 – Example coil and former (C)

Here L is given in μH with $a = (r_o + r_i)/2$ the distance from the centre of the coil to the centre of the windings, $c = r_o - r_i$ the difference between inner and outer radii of the coil and l the length of the coil all in units of mm and seen in figure 5, N is the number of turns. This approximation is accurate to within 1% when the the coil cross section is roughly square, which is true for all but one of our coils. The program was used iteratively to find the length of the coil required to give outer radii in the desired range given the properties we have discussed and the copper wire gauges available. Table 2 details the properties of the final designs. Once the coils have been built it will be a simple matter to measure their inductances and resistances (at 77K) and add the appropriate resistors in series.

2.3 Coil Construction

To wind the coils formers had to be constructed. The basic construction of a former is a rod the diameter of the desired bore size with two end cheeks to support the coil. The material these were made of had to withstand the following: being rapidly cooled to liquid nitrogen temperatures, outward stress on the end cheeks due to tightly wound coils and stress due to forces produced during the pulse. Also, as the former would be present during the magnetisation for support, it had to be non-magnetic as during a pulse it should not substantially alter the field generated.

The former also needed to hold the Hall probe and the pick up coil which will be used to measure the fields during and after a pulse. The specifications for the Hall probe mount are that the Hall probe must be held at the center of the sample (±1mm) and must not be allowed to move, the Hall probe itself must be protected from being crushed between the coil and sample during a pulse and must be easily transferable between different coils.

The design we came up with (see figure 5) for each coil in a split coil pair was as follows. One substantial end cheek 20mm in thickness and one thinner end cheek which sits next to the sample. As we wanted to maximise the field at the sample we wanted to minimise the distance between the coil and the sample and so we made a circular inset, the same diameter as the largest sample, into the thinner cheek to not only bring the sample closer to the coil but also hold it central. A further circular inset was made in the centre of the former required to hold the Hall probe, it was made slightly deeper than the thickness of the Hall probe and a groove was machined from the centre to the outside at that depth with which to contain the wires for the probe and pick up coil. The Hall probe was mounted carefully to a circular piece of Tufnol grade 6F45 cotton epoxy and a groove was cut around the perimeter of the cylinder into which we wound the pickup coil. This was made of copper wire, 15 turns were wound in a radius of 7.5mm. This circular disk was then itself mounted in a piece of Carp brand Tufnol seen in figure 3 on which the wires were fixed (2 for the pickup coil, 4 for the Hall probe, 2 for the power input and 2 for the output).

The bore was a smooth cylinder that was threaded at the ends to be glued into the end cheeks. Holes were drilled into the end cheeks at the position of the innermost and outermost winding for

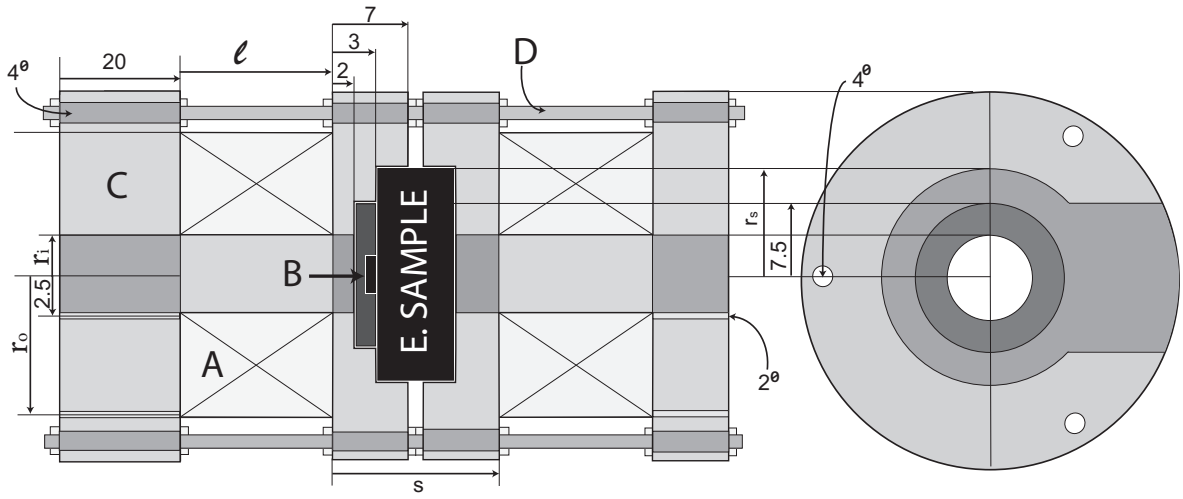

Figure 5 – Left: General cross section of Tufnol 6F45 former (C), split coil (A) and sample (E), showing position of Hall probe (B). Also shown are the brass supports (D) with holding nuts. Right: view of end cheek with sample and Hall probe mount insets (darker shading represents greater depth). l , r_i and r_o are the length, inner and outer radius of the coil, and r_s is the radius of the largest sample. Measurements in mm.

the winding wire to be passed into and out of the former. To secure the pair of coils into the split arrangement 3 holes were made through the four cheeks into which threaded brass bar was inserted. These holes on the uppermost cheek were threaded and the rest were clearance holes with nuts used to hold the cheeks in place.

A former was machined out of nylon to test the design, there were some minor problems machining nylon as the material is quite malleable, but the coils were successfully wound to within an acceptable accuracy of the specifications. We found that each layer we wound we under-wound by 1 and 2 turns, we therefore decided to extend the length of the formers by two times the diameter of the wire so that we could fit the number of turns we had planned into the coil. We used a thin layer ($0.1mm$) of pre-impregnated composite fiber between each layer of windings. These were impregnated with epoxy resin, which upon baking at 100C for 3 hours bonds the windings together and further help resist the Lorentz forces present during pulses.

After the resin was cured the coils were fitted together and tightened. Tests and full sets of pulses were performed on the split coil showing that it was able to function under the conditions imposed by the cryogenic pulsing up to $V_{cap} = 60$V.

All subsequent formers were made out of Tufnol grade 6F45 cotton epoxy for the end cheeks and Tufnol grade 10G40 glass epoxy for the bores of the formers. These materials were chosen for their mechanical strength, dimensional stability and, in the case of 6F45, its excellent machining properties [27].

2.4 Experimental set up

The critical temperature of GdBCO is 92.9K [28] allowing the experiment to be conducted in liquid nitrogen (77K). The Hall probe HHP-NP (specification available from AREPOC [29]) has an active area of 0.625mm and is supplied with its nominal control current (20mA) by a low drift constant current supply. There are 3 quantities to be logged, the Hall probe output voltage, the pickup coil voltage, and the current flowing through the coils. These were logged using a high precision data logger (NI 6281) running at 1 kilo-sample per second. The pick up coil was used as a backup, if trouble was had with the Hall probe.

The procedure for a run is as follows: A sample and Hall probe are placed into the desired coil. The former is then tightened and cooled down to 77K using a bath of liquid nitrogen. Once it has cooled and nitrogen returns to a normal level of boiling, the capacitor is charged and pulsing can begin. After a run of pulsing the sample is taken out of the liquid nitrogen, raising it above its critical temperature (within 10 minutes) where it stops superconducting and looses its trapped flux. This process can then be repeated.

3 Results and discussion

I will now detail the results of this experiment. First I will look at the preliminary results, including the properties of the constructed coils, and then move on to the multi-pulse runs and the interpretation of the results.

3.1 Preliminary results

3.1.1 Hall Probe Calibration

The high sensitivity Hall probe used came pre-calibrated with a sensitivity of 109.6mV/T at room and cryogenic temperatures. A calibration was performed after our experiment was complete to check if there was a drift in the calibration.

Coil D supplied a magnetic field and a Gauss meter was used to measure the magnetic field at the position of the Hall probe. This method gave a calibration of 120.6 ± 3.0mV/T which shows a considerable drift. It is hard to account for this in the results as it is unclear which calibration is more suitable for a given measurement. I will include this possible discrepancy in calibration as part of my errors.

3.1.2 Manufactured coils properties

Measurements of the inductance and resistances of the coils were performed using a Wayne Kerr LCR meter, at room temperature and at 77K. Measurements were carried out for all sample-coil combinations as the separation of the split coil pair changes with sample, however this was found to be a very small effect on the inductance (maximum $< 3\%$). The inductances measured were all significantly less than planned, and there was considerable variation ($\pm 14\%$) between the coils' inductances. This can be attributed to the winding process which is an inexact art with such small coils. Not only was there trouble fitting in the specified amount of turns, even with the excess planned for, often it was found that there would be edge defects whereby layers would taper at the ends due to inexact winding throughout the layer. There were other factors that could not be accounted for in the program we used to design the coils, for example the wire structure and composite fiber layers, so it was expected that the inductance would be reduced.

After some preliminary tests on coil A we found that it was very inefficient at trapping flux due to its short rise time, high resistance and therefore low peak current and field. It was decided that matching the resistances of the other coils to this would decrease the maximum flux trapped significantly for all the coils and so it was decided that when matching the resistances of the coils A should be ignored. This meant increasing the resistance of C and D to that of B.

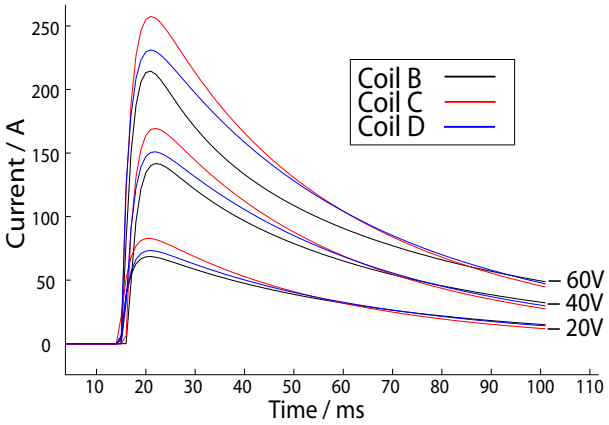

Figure 6 – Pulse shapes as measured through the shunt resistor for the coils with resistances equalised. Pulses for different coils have approximately the same characteristics.

A summary of the coil properties is given in table 3. Notice that after resistances are added the rise times of the three coils are closely matched. The peak field is also somewhat more similar after resistors are added, this is due I_{max} becoming equalised.

3.1.3 Pulse shapes

Upon measuring $\gamma = \alpha^2/\omega_0^2$ (section 2.1) it was found that all the coil setups were in the over damped regime (as predicted) except for Coil D without the additional resistors which, due to its low resistance was in the under damped regime. This affected the subsequent decay of the pulse as approximating the circuit as an LR circuit (as in equation 4) is not valid. The lengths of these pulses is therefore shorter than in the over damped cases.

It was found that once the rise times had been matched (and therefore the peak current) all pulses had a similar shape and duration (see figure 6) allowing, at least in this respect, comparisons to be made between different coils independent of these factors. It should be noted however that [25, Fig 7] shows that for rise times below 15ms, small changes in rise time can have a dramatic effect on the field trapped, and so even though our rise times are closely matched, small discrepancies could cause large departures in trapped flux.

Coil	A	B	C	D	errors
Inductance/μH	466	416	359	390	
Resistance / Ω	0.350	0.211	0.111	0.045	5
Average rise time / ms	5.1	6.1	7.2	9.5	$\pm$2
Peak magnetic field / T	0.180	0.756	0.980	1.124	$\pm$0.01
With added resistance					
Resistance / Ω		0.211	0.211	0.195	$\pm$0.01
Average rise time / ms		6.1	6.2	6.3	$\pm$2
Peak magnetic field / T		0.7560	0.7899	0.4886	$\pm$0.01

Table 3 – Measured inductances and resistances of the 4 coils at $T = 77$K and measured rise times resulting. Peak magnetic field produced (at $V_{cap} = 60$V) using measured I_{max} and numerical integrator Bsol.

3.1.4 B applied

It is important to know the maximum magnetic field that is applied during a pulse, as for each different combination this will vary. The peak magnetic field measured by the Hall probe is partly shielded by the sample during a pulse and therefore is not a reasonable representation of the peak applied field. The most reliable technique of calculating this quantity is to use the logged current through the coil and calculating the max magnetic field due to the split coil using a numerical simulation program (Bsol [30] was used) or the analytical expression for the field at the centroid of a split coil (equation 6), the starting point for the derivation can be found in [20, p226].

$$B = \mu_0 J_L r_i \left\{ \beta \ln \left[\frac{\alpha + \sqrt{\beta_1^2 + \alpha^2}}{1 + \sqrt{1 + \beta_1^2}} \right] - \beta_2 \ln \left[\frac{\alpha + \sqrt{\beta_2^2 + \alpha^2}}{1 + \sqrt{1 + \beta_2^2}} \right] \right\} \quad (6)$$

With the current density J_L where the parameters are given by $\alpha = r_o/r_i$, $\beta_1 = (2l + s)/4r_i$, $\beta_2 = s/r_i$ with r_o and r_i the outer and inner radius of the coil, l the length of one coil and s the separation of the coils as seen in figure 5.

It was found that results of the numerical simulation program Bsol agreed well with the above equation, and so Bsol was used to give the field at the position of the Hall probe. The applied magnetic field is proportional to the current supplied and is therefore highly dependent on the coil properties, in particular the resistance of the coil (see table 3).

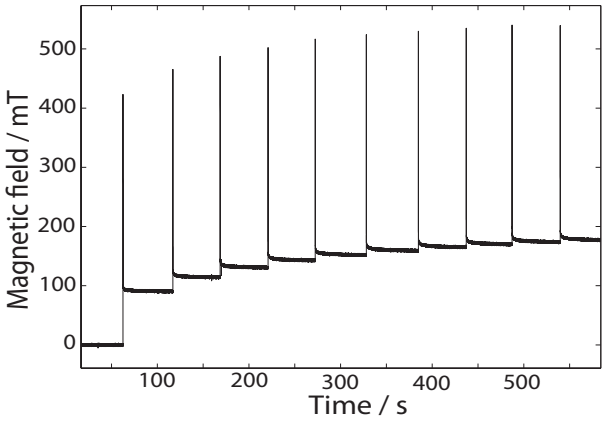

Figure 7 – A Hall probe reading of a 10 pulse run. Sample 2, Coil D, $V_{cap} = 50$V

3.2 Runs of pulses

Two sets of runs were performed. First a complete set of pulses on all sample and coil combinations with V_{cap} ranging from 10V to 60V (in 10V increments). Then the same was carried out after adding resistors in series with the coils to equalise the rise times (this time in 20V increments in V_{cap} were used due to time constraints). This is a total of 90 different runs each with 10 pulses performed (typical run see figure 7). I will now discuss the features of these runs and the results obtained.

3.2.1 Time between pulses

It was decided that each run should involve a primary pulse and then a succession of nine pulses, this was enough to see the effect the secondary pulses had on final trapped flux and consider extrapolating a trapped field saturation limit. The saturation is caused by two effects, there is a maximum amount of trapped flux for a given sample-magnetic field combination (HTSC have been seen to trap upward of 95% field applied [16] using other trapping techniques) and the effect of thermally activated flux creep between pulses, in which the trapped field de-

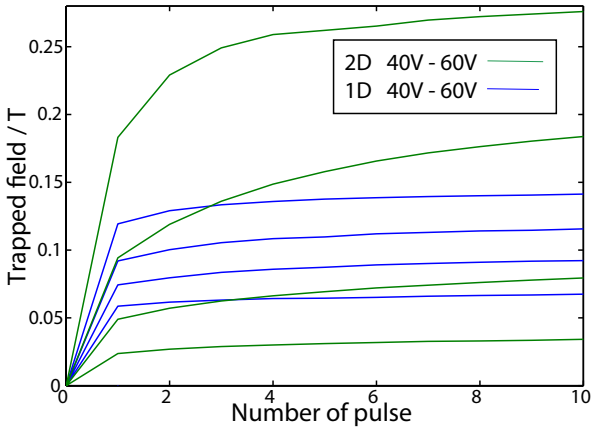

Figure 8 – A graph showing the flux trapped after each pulse in a 10 pulse run for coil D samples 1 (blue) and 2 (green). Runs with higher V_{cap} (ranging from 30V to 60V) are seen to trap more flux.

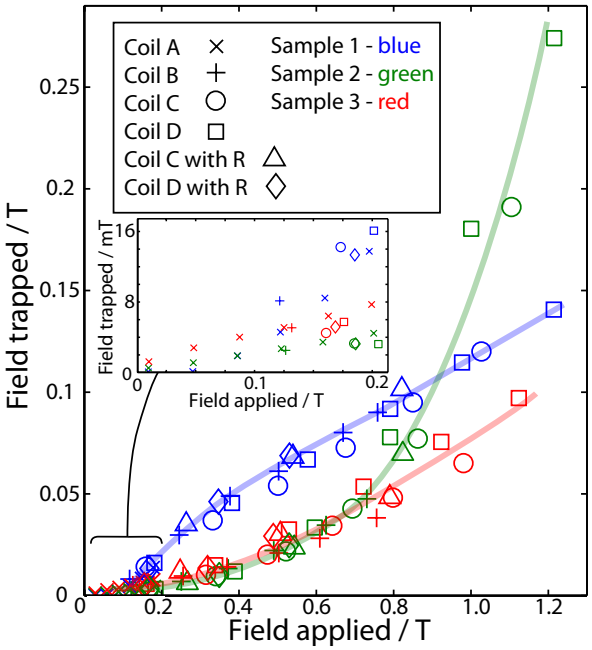

Figure 9 – Final trapped field against field applied for all runs with inset magnifying the range from 0-0.2T applied field. Lines illustrate apparent trends for each sample and are guides only. Overlapping of points from different coils suggests little dependence of the flux trapped on the coil used (see section 3.2.4).

cays after the initial trapping. It is therefore important to minimise the time between successive pulses.

It was decided to fire the capacitor as soon as the voltage across it was 99% that of V_{cap}. The speed at which these pulses could be fired depends on the time taken to charge the capacitor bank, which in turn depends on the V_{cap}. This time varied between 20s for $V_{cap} = 10$V and 70s for $V_{cap} = 60$V. Another method which was tested was to wait a set amount of time (70s so that the capacitor would always be fully charged) between firing pulses, but this caused flux creep to have the greatest effect on the runs that trapped the least flux (i.e. $V_{cap} = 10$V) so it was decided to fire the capacitor as soon as it was charged to 99% independent of V_{cap}, limiting the dissipation of trapped flux due to flux creep and thus maximising the maximum trapped flux.

3.2.2 The relation between the first pulse and subsequent pulses

It is interesting to remark that in most cases the first pulse traps a high proportion of the final trapped flux, an average of $\sim$ 80% for both runs with and without resistors. It was found that this proportion decreases with increasing V_{cap} starting at $\sim$ 90% with $V_{cap} = 10$V and decreasing to $\sim$ 75% at $V_{cap} = 60$V showing that in increasing V_{cap} allows more flux to be trapped on subsequent pulses for the same sample.

There are some combinations, notably sample 2 with coils C and D before adding resistors, that have a significantly smaller proportion trapped on their first pulse with D dropping dramatically to a minimum of $\sim$ 50% when the $V_{cap} = 60$V. It is on these runs that the highest amount of final trapped flux is found.

Figure 8 shows runs of 10 pulses with combinations 1D and 2D without added resistors. The 1D runs are fairly typical, trapping a large proportion of the flux of their first pulse, where as it is seen that the 2D runs trap a much smaller proportion on their first pulse and allow for considerable flux to be trapped on the subsequent pulses.

3.2.3 Relationship of field trapped to field applied for different samples

It was found that sample 1 (small diameter) consistently trapped more flux for an applied field than other samples in the low field regime (< 0.8T), with the field trapped increasing fairly linearly with that applied (see figure 9). However above this field sample 2 (larger diameter) is found to be the best flux trapper, displaying a dramatic increase in efficiency at high field. At the highest field in this study sample 2 traps the largest flux (260mT) with the highest efficiency (21% of applied pulse field was trapped). Sample 3, which is thicker, performs in a similar manner to sample 2 below 0.6T, but then departs from samples 2's large increase in efficiency at high fields.

Other studies that have observed the dependence of the flux trapped in a sample on the applied field (notably [31, 32] which compare different methods

of magnetisation). These find relationships in which the trapped flux increases with applied field, reaches a maximum then slowly decreases due to flux line movement and heating [33]. The data presented here lies in the increasing range, the field being too small to observe the plateau and subsequent decrease in trapped flux. Other studies mentioned here do not show the dependence of field trapped at low applied fields in as much detail as here, so the different shapes of sample curves seen in figure 9 can not be compared to the literature.

3.2.4 Relation of relative coil diameter and sample diameter to flux trapping

Figure 9 displays a strong relationship for each sample between the applied field and the field trapped which is not very dependent on the coil arrangement used (at least within reasonable errors margins of this experiment). This is noted by observing that there is close overlap of many points from the same sample coming from different coil arrangements (points with same colour, different symbols). These runs apply approximately the same field and trap roughly the same flux highlighting that the flux trapped depends mainly on the applied field and sample rather than other factors like the coil used. These points occur at low applied fields (<0.8T) where many runs with different coils were performed, at high fields less runs were performed and it is not possible to draw such conclusions.

As there is such a strong dependence on the applied field an attempt was made to compare, in detail, runs with approximately the same field applied. Unfortunately, as the runs weren't planned to apply the same fields very few did. A study was carried out on the few runs in which the applied field was roughly similar, however the interpretation of the results were inconclusive. Many show that if the applied field is even slightly higher the trapped flux will be higher dwarfing any other possible effect that may be present due to coil sample geometry and others don't provide a statistically conclusive result.

As the flux trapped is not significantly dependent on the coil used, a relationship between the ratio of coil and sample diameters to the flux trapped (as in [18]) is not observed.

4 Conclusions

Four split coils were produced, all of different outer diameters, to magnetise three bulk GdBCO superconducting samples using the pulse field magnetisation (PFM) technique. An investigation was undertaken into the effect of varying the relative diameter of the coil and the sample on the flux trapping capabilities of the arrangement. The results from this study, which involved 90 sets of 10 pulse runs, applying a peak field ranging from 28mT to 1.21T show some interesting, but inconclusive results.

In Xu's paper [18] simulations were carried out that showed an increase in flux trapping potential of a coil-sample combination when the ratio between the diameters of coil and sample were between 0.5 and 1. In this study clear evidence of a relationship of this nature was not observed however observations do suggest a number of avenues for further investigation.

This study showed that the magnetisation was very sample dependent with the smallest diameter sample (sample 1) out performing the other samples independent of the coil used for low applied fields < 0.8T. Sample 1 is also observed to have a fairly linear relationship between the field applied and field trapped in the regime studied, whereas the relationship in the case of sample 2 is very non-linear, trapping substantially more flux at higher applied fields. This dependence on the sample, may be due to the mechanism of flux penetration in samples of different dimensions, or may be due to the individual quality of the samples. As the results were very sample dependent, comparisons to Xu's work [18] were challenging.

There are many possible extensions to this work that could be carried out to address several of the problems encountered:

The applied field had a large effect on the flux trapped, therefore to further this experiment it would be informative to carry out a full study on a series of runs that apply the same field. This could be achieved by varying V_{cap} to give the same field among several coils. Careful study of these runs could show relationships between coil sample diameters and trapped flux that cannot be resolved with the data available in this study.

Carrying out the optimisation problem mentioned in section 2.2 for designing coils of the same rise time and similar (and maximal) peak fields would be of great value as this may lead to coils produced with similar properties and studies of runs applying the same field may be conducted at higher fields.

Different flux trapping relationships may be observed at higher fields (higher fields could be achieved by using a capacitor bank with higher allowed V_{cap}). It would be of interest to see if sample 3 follows sample 2's flux trapped - flux applied characteristic at high enough field, this may support the conclusion that higher applied fields are required to fully penetrate thicker samples.

A greater selection of coil and sample diameters would have improved this study as with so few sample to coil diameter ratios available drawing meaningful conclusions is very difficult.

A further extension to the experiment would be to look at the effect of lowering the temperature below that of liquid nitrogen, this could increase the trapped field as in [34] in which decreasing the temperature from 77K to 20K increased trapping by 600%.

Using a scanning Hall probe would allow for analysis of field trapped across the whole sample surface and not just at the centre. This would give a more accurate representation of the flux trapped as the distribution of flux across the sample can have a variety of profiles for different trapping techniques [21, 22, 35]. The total flux trapped in the sample could also be found and comparisons between samples of different volume could be made more effectively.

5 Acknowledgments

Special thanks to Richard Lewin for his advise and expertise and Tony Hickman for his help in the workshop.

References

[1] H. Fujishiro, T. Tateiwa, A. Fujiwara, T. Oka, H. Hayashi, “Higher trapped field over 5 on HTSC bulk by modified pulse field magnetizing” Physica C, 445–448 (2006), p. 334

[2] Masson, P.J.; Luongo, C.A.; , “High power density superconducting motor for all-electric aircraft propulsion,” Applied Superconductivity, IEEE Transactions on , vol.15, no.2, pp. 2226- 2229, June 2005 doi: 10.1109/TASC.2005.849618

[3] Yoshitaka Itoh, Yousuke Yanagi, Masaaki Yoshikawa, Tetsuo Oka, Shintaro Harada, Tsutomu Sakakibara, Yuh Yamada, Uichiro Mizutani “High-Temperature Superconducting Motor Using Y-Ba-Cu-O Bulk Magnets” Jpn. J. Appl. Phys. 34 (1995) 5574

[4] Ohsaki, H Terao, Y Sekino, M ”Wind turbine generators using superconducting coils and bulks”, Journal of Physics Conference Series, Vol.234, Iss.3, pp.032043, 2010, ISSN: 17426588

[5] Miyagawa Y, Kameno H, Takahata R and Ueyama H 1999 IEEE Trans. Appl. Supercond. 9 996

[6] Ohashi S, Tamura S and Hirane Y 1999 IEEE Trans. Appl. Supercond. 9 988

[7] A Patel et al 2011 Supercond. Sci. Technol. 24 015009 doi:10.1088/0953-2048/24/1/015009

[8] Kim, S. B.; Imai, M.; Takano, R.; Joo, J. H.; Hahn, S. “Study on Optimized Configuration of Stacked HTS Bulk Annuli for Compact NMR Application” IEEE Transactions on Applied Superconductivity, vol. 21, issue 3, pp. 2080-2083 DOI: 10.1109/TASC.2010.2089590

[9] H. K. Onnes, Comm. Phys. Lab. Univ. Leiden, Ãos. 119, 120, 122 (1911)

[10] J.G. Bednorz, K.A. Müller Z. Phys. B, 64 (1986), p. 189

[11] M. K. Wu, J. R. Ashburn, C. J. Torng, “Superconductivity at 93 K in a new mixed-phase Y-Ba-Cu-O compound system at ambient pressure” Phys. Rev. Lett. 58, 908–910 (1987)

[12] Meissner, W.; R. Bochsenfeld (1912). ”Ein neuer Effekt bei Eintritt der Supraleitfähigkeit”. Naturwissenschaften 21 (44): 787–788. Bibcode 1933NW.....21..787M. doi:10.1007/BF01504252.

[13] J. F. Annet; “Superconductivity, superfluids, and condensates”, Oxford University Press (2004)

[14] G. Krabbes, G. Fuchs, W.-R. Canders, H. May, R. Palka, High temperature superconductor bulk materials, Wiley-VCH Verlag GmbH & Co. KGaA. (2006).

[15] A.A. Abrikosov, Soy. Phys . JETP 32, 1444 (1957)

[16] Tomita, Masaru AU, Murakami, Masato TI, “High-temperature superconductor bulk magnets that can trap magnetic fields of over 17 tesla at 29K” Nature 421, 517-520 (2003) | doi:10.1038/nature01350

[17] Y Jiang, R Pei, W Xian, Z Hong and T A Coombs "The design, magnetization and control of a superconducting permanent magnet synchronous motor" Supercond. Sci. Technol. 21 065011 doi:10.1088/0953-2048/21/6/065011

[18] Zhihan Xu, Richard Lewin, Archie M Campbell, David A Cardwell and Harry Jones 2012 Supercond. Sci. Technol. 25 025016 doi:10.1088/0953-2048/25/2/025016

[19] D.V. Bugg "Electronics: circuits, amplifiers and gates" Institute of Physics Publishing, 1991; ISBN: 0750301090

[20] D.B. Montgomery, "Solenoid Magnet Design" (Robert E. Krieger 1980) SBN: 471 61403

[21] Ida T et al 2004 Physica C 412–414 638

[22] Kamijo, H.; Fujimoto, H.; , "Repeated pulsed-field magnetization with temperature control in a high-Tc bulk superconductor," Applied Superconductivity, IEEE Transactions on , vol.11, no.1, pp.1816-1819, Mar 2001 doi: 10.1109/77.920200

[23] Kimura Y, Matsuzaki H, Ohtani I, Morita E, Izumi M, Sakai N, Hirabayashi I, Miki M, Kitano M and Ida T 2006 Supercond. Sci. Technol. 19 S466

[24] Fujishiro H, Naito T and Oyama M 2011 Supercond. Sci. Technol. 24 075015

[25] Ishigohka, T.; Ichikawa, H.; Ninomiya, A.; Kamijo, H.; Fujimoto, H.; , "Flux trapping characteristics of YBCO bulks using pulse magnetization [superconducting magnets]," Applied Superconductivity, IEEE Transactions on , vol.11, no.1, pp.1980-1983, Mar 2001 doi: 10.1109/77.920241

[26] Wheeler, H.A.; , "Simple Inductance Formulas for Radio Coils," Proceedings of the Institute of Radio Engineers , vol.16, no.10, pp. 1398- 1400, Oct. 1928 doi: 10.1109/JRPROC.1928.221309

[27] Tufnol Composites, www.tufnol.com

[28] Toshihiro Iguchi et al 2002 Supercond. Sci. Technol. 15 1415 doi:10.1088/0953-2048/15/10/309

[29] Arepoc, Specification of high sensitivity Hall probes - http://www.arepoc.sk

[30] P.E. Richens Oxford University DPhil Thesis 2000 'Bsol'

[31] U. Mizutani, T. Oka, Y. Itoh, Y. Yanagi, M. Yoshikawa, H. Ikuta, "Pulsed-field magnetization applied to high-Tc superconductors", Applied Superconductivity, Volume 6, Issues 2–5, February–May 1998, Pages 235-246, ISSN 0964-1807, 10.1016/S0964-1807(98)00106-9

[32] H. Ikuta, H. Ishihara, T. Hosokawa, Y. Yanagi, Y. Itoh, M. Yoshikawa, T. Oka, and U. Mizutani, Supercond. Sci. Technol. 13, 846 ~2000

[33] S. Braeck, D. V. Shantsev, T. H. Johansen, and Y. M. Galperin, "Superconducting trapped-field magnets: Temperature and field distributions during pulsed-field activation" J. Appl. Phys. 92, 6235 (2002), DOI:10.1063/1.1515098

[34] X Chaud, E Haanappel, J G Noudem and D Horvath, "Trapped field of YBCO single-domain samples using pulse magnetization from 77K to 20K," X Chaud et al 2008 J. Phys.: Conf. Ser. 97 012047 doi:10.1088/1742-6596/97/1/012047

[35] D.A. Cardwell, M. Murakami, M. Zeisberger, W. Gawalek, R. Gonzalez-Arrabal, M. Eisterer, H.W. Weber, G. Fuchs, G. Krabbes, A. Leenders, H.C. Freyhardt, X. Chaud, R. Tournier, N. Hari Babu, "Round robin measurements of the flux trapping properties of melt processed Sm–Ba–Cu–O bulk superconductors", Physica C: Superconductivity, Volumes 412–414, Part 1, October 2004, Pages 623-632, ISSN 0921-4534, 10.1016/j.physc.2004.01.082.